

13 Trapping and Cooling

Whereas first single atom experiments exploited dilute atomic beams, modern approaches investigate trapped atoms. One distinguishes between traps for charged atoms, i.e. ions and traps for neutral atoms.

13.1 Ion traps

13.1.1 Paul traps

It is well known from the so-called Earnshaw theorem that a charged particle cannot be trapped in a stable configuration with static electric fields only. However, a combination of static electric and magnetic fields (**Penning trap**) or time dependent electric fields (**Paul trap**) can provide space points where a restoring force in all three directions acts on a charged particle.

A Paul trap (Nobel Prize 1989) consists of two parabolical electrodes and a ring electrode.

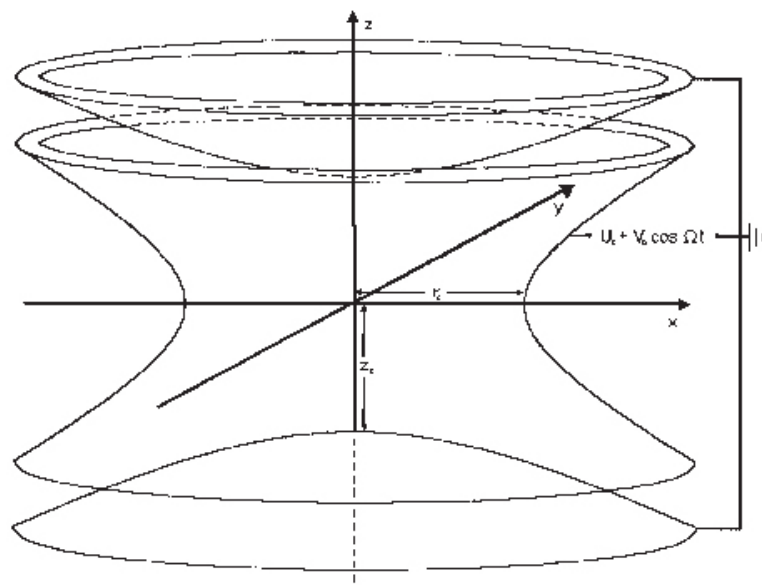


Figure 105: Sketch of a Paul trap

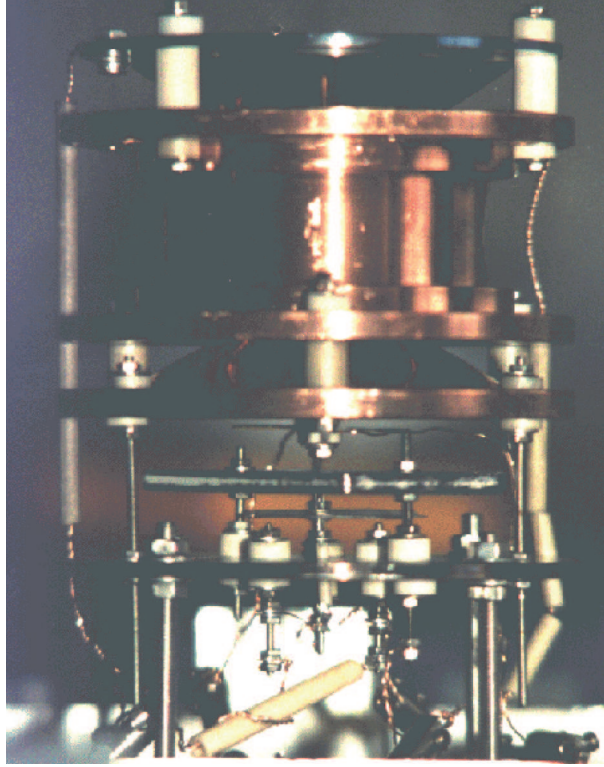


Figure 106: Photo of a Paul trap [from <http://www.physik.uni-mainz.de>]

If a dc-voltage U_{dc} and an ac-voltage V_{ac} of frequency Ω is applied to the electrodes then the potential near the trap axis is of the form:

$$\Phi = \frac{(U_{dc} + V_{ac} \cos(\Omega t))(r^2 - 2z^2 + 2z_0^2)}{r_0^2 + 2z_0^2}$$

where r_0 and z_0 denote the distances from the trap axis to the surface of the electrodes.

The potential is harmonic and for a certain time t provides a restoring force in one dimension.

Say, at a given time t the x-direction is the non-confining direction. Then, due to its inertia a particle cannot escape along that direction before the sign of $\cos(\Omega t)$ is inverted, and the x-direction becomes the confining direction. For certain frequencies Ω this results in an effective confinement in all three directions.

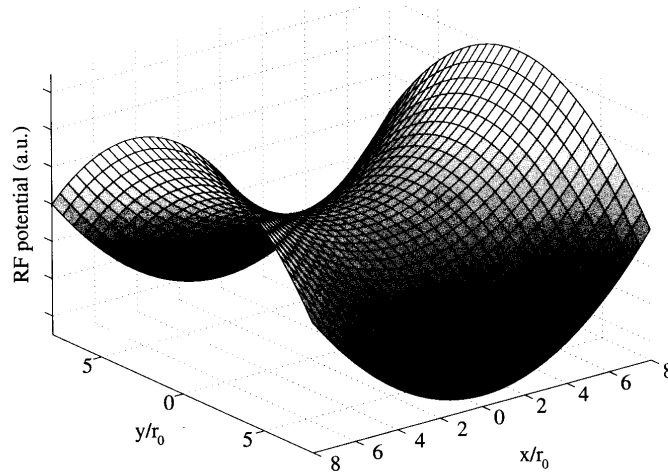


Figure 107: Paul trap potential [from Bouwmeester et al.]

The equations of motion in a Paul trap are:

$$m \frac{d^2}{dt^2} \begin{pmatrix} x \\ y \\ z \end{pmatrix} = \frac{2q(U_{dc} - V_{ac} \cos(\omega t))}{r_0^2 + 2z_0^2} \begin{pmatrix} -x \\ -y \\ 2z \end{pmatrix}$$

With the transformation

$$\begin{aligned} \tau &= 1/2\omega \\ a_x &= a_y = -a_z/2 = \frac{4qU_{dc}}{mr_0^2\Omega^2} \\ q_x &= q_y = -q_z/2 = \frac{2qV_{ac}}{m\Omega^2r_0^2} \end{aligned}$$

one finds the *Mathieu equations*:

$$\frac{d^2 u_i}{d\tau^2} + (a_i + 2q_i \cos(2\tau)) u_i = 0$$

with $i = x, y, z$

For the approximation $a_i < q_i \ll 1$, which is usually fulfilled, there exists an analytic solution:

$$u_i(t) = A_i \cos(\Omega_i t + \phi_i) \left[1 + \frac{q_i}{2} \cos(\omega t) \right]$$

The solution consist of a rapid oscillation with the trap frequency ω , the so-called *micromotion*, and a slower *macromotion* (or *secular motion*) at frequency Ω_i in the effective harmonic trap potential with:

$$\Omega_i \approx \frac{\omega}{2} \left(a_i + \frac{q_i}{2} \right)$$

In the trap center the micromotion vanishes completely.

As an example of a very fundamental experiment with single trapped ions Fig. 109 shows the fluorescence from a single Ba-Ion.

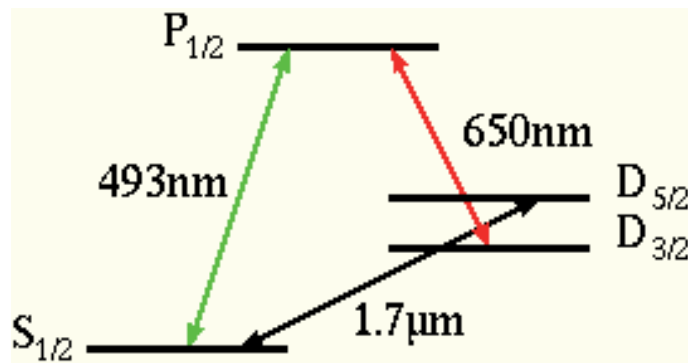


Figure 108: Energy levels of Ba

If a single ion is trapped and continuously illuminated with laser light (here on the $P_{1/2} \rightarrow S_{1/2}$ transition, see Fig. refBalevels) then the fluorescence vanishes abruptly due to transitions to the metastable $D_{5/2}$ level (The other arrow indicates repumping from the $D_{3/2}$ level). First experiments were performed in 1986. The possibility to observe these "Quantum Jumps" led to many theoretical discussions in the early 50's.

13.1.2 Trapping ion strings

In order to realize well-controllable experiments several ions the Paul trap has to be modified to *Linear ion traps*. These traps usually consist of two pairs of electrodes (hyperbolically shaped, spherical rods, or rectangular shapes) which provide a confinement in two directions. These configurations resemble mass spectrometers (more precisely e/m filters). A second pair of end cap electrodes provides the confinement in the orthogonal direction. Figure 110 shows various configurations.

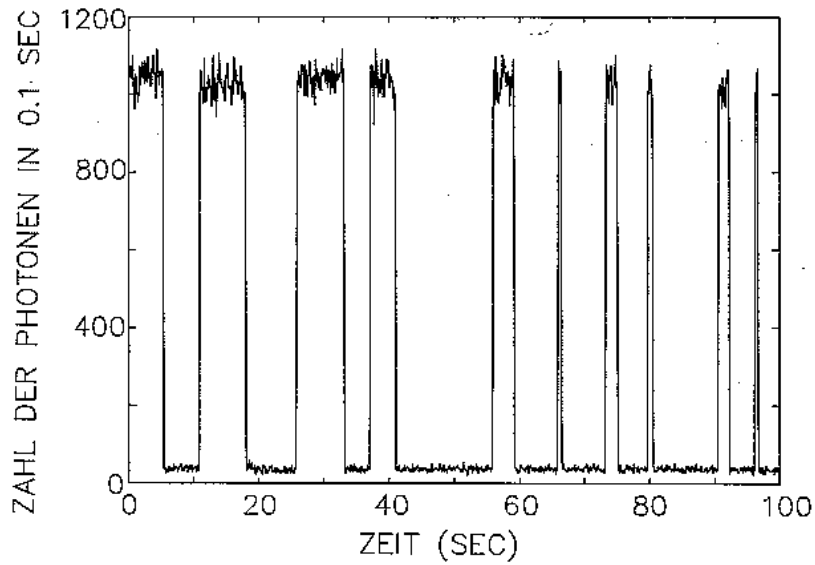


Figure 109: Quantum jumps of a single Ba-atom[from <http://www.physnet.uni-hamburg.de/ilp/toschek/ionen.html>]

In a linear trap the equation of motion in z-direction (direction of the end caps) is given by:

$$\frac{d^2 u_z}{dt^2} + (2\kappa q U_{cap} / m z_0^2) u_z = 0$$

where q, m are the charge and mass of the ion and κ is an empirically found parameter.

The equation of motion in the orthogonal directions is given again by the Mathieu equations:

$$\frac{d^2 u_i}{d\tau^2} + (a_i + 2q_i \cos(2\tau)) u_i = 0$$

with $i = x, y$

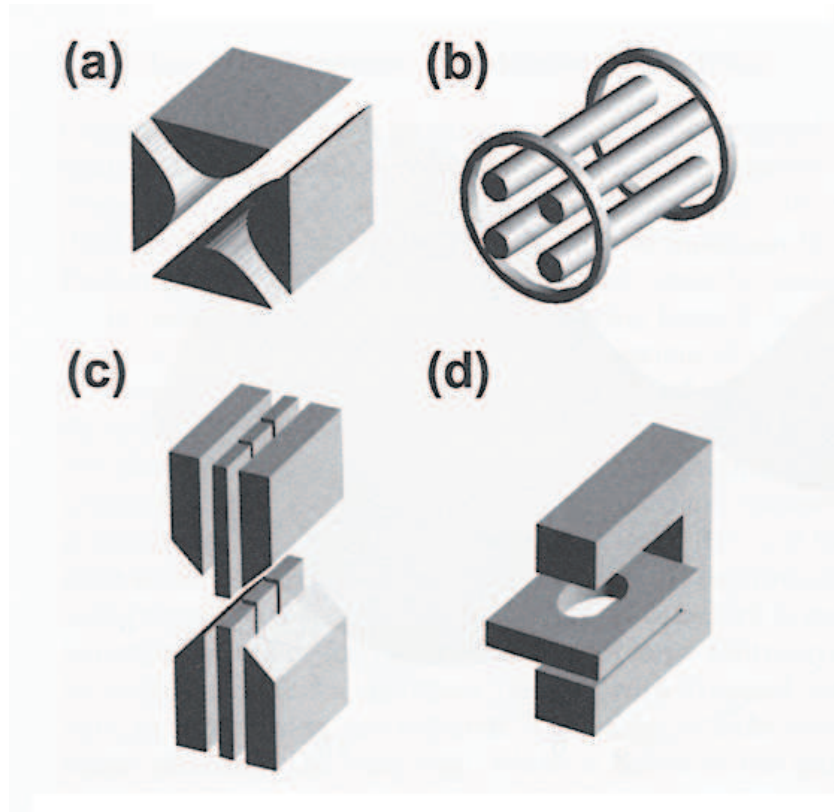


Figure 110: Different types of linear ion traps [from Bouwmeester et al.]

where

$$\begin{aligned}
 a_x &= \frac{4q}{m\Omega^2} \left(\frac{U_{dc}}{r_0^2} - \frac{\kappa U_{cap}}{z_0^2} \right) \\
 a_y &= -\frac{4q}{m\Omega^2} \left(\frac{U_{dc}}{r_0^2} + \frac{\kappa U_{cap}}{z_0^2} \right) \\
 q_x &= -q_y = \frac{2qV_{ac}}{m\Omega^2 r_0^2} \\
 \tau &= \Omega t / 2
 \end{aligned}$$

Similar as in the single-ion trap the motion of the ions can be approximated as a combination of micro- and macromotion. What is important now is that *the micro-motion vanishes completely on the whole trap axis!*

Figure111 shows a collection of pictures (raw video data) of stored Ca-ion strings.

The images were taken with CCD cameras:

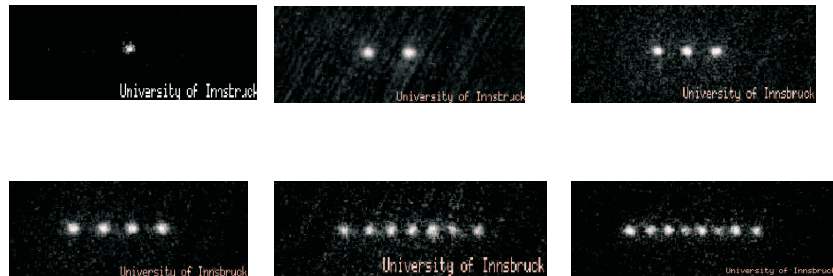


Figure 111: Strings of ions stored in a linear Paul trap [from <http://heart-c704.uibk.ac.at/>]

13.1.3 Normal Modes

If the radial confinement in a linear ion trap is strong enough, ions arrange in a linear pattern along the trap axis at low temperatures. The distance between the ions is determined by the equilibrium of the Coulomb repulsion and the potential providing axial confinement.

Small displacements of the ions from their equilibrium position cannot be described in terms of the motion of individual ions since the Coulomb interaction couples the charged particles. Instead, the motion of the string must be described in terms of *normal modes*.

- One example of a normal mode is the *center-of-mass* (COM) mode of the string. This corresponds to an oscillation of the whole string as if all ions were rigidly joined.
- Another example is the *breathing mode*. It describes an oscillation where the ions move in opposite directions and leave the COM fixed.
- The spectrum of other higher order modes can be calculated from the trap parameters.

The following figure shows the experimental observation of the COM mode and the breathing mode of a string of 7 Ca atoms which were excited via the trap's end cap electrodes:

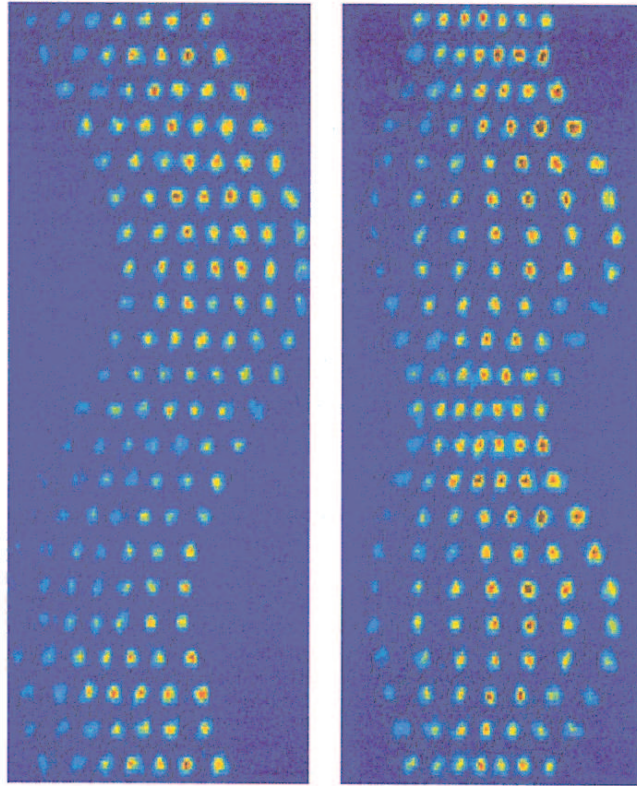


Figure 112: Excitation of normal modes in a string of 7 Ca atoms [from Bouwmeester et al.]

13.2 Laser Cooling

If a string of trapped ions should be used for quantum computation it is required to cool ions down to the ground state of their normal modes. (More recent proposals have weakened this requirement, but cooling is yet desirable).

With laser cooling (Nobel prize for Chu, Cohen-Tannoudji, Phillips) temperatures which are far beyond reach of cryostats could be realized.

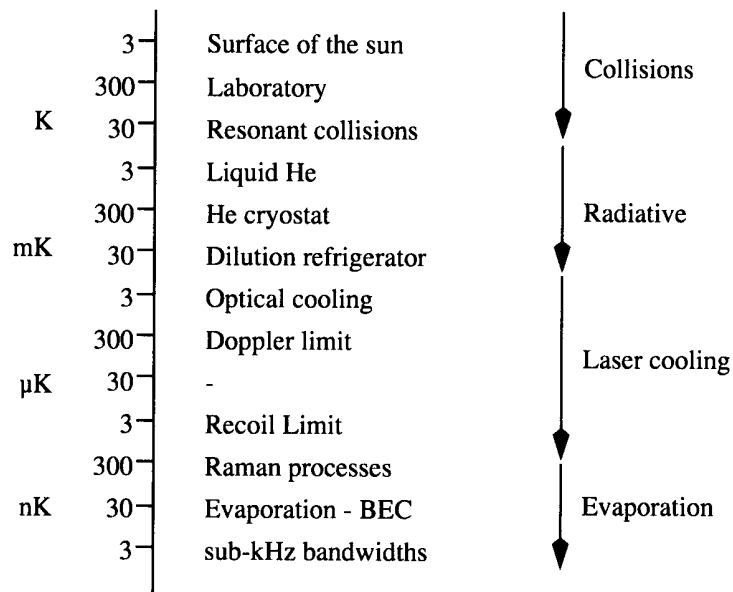


Figure 113: Temperature scale [from H. J. Metcalf, P. van der Straten, "Laser Cooling and Trapping", Springer N.Y. 2002]

The definition of "temperature" in laser cooling requires some discussion. It is used to describe an atomic sample whose average kinetic energy $\langle E_k \rangle$ has been reduced by laser cooling. The label "temperature" now is written as:

$$\frac{1}{2}k_B T = \langle E_k \rangle$$

with Boltzmann's constant k_B .

13.2.1 Doppler Cooling

The idea of laser cooling is illustrated by the following figure:

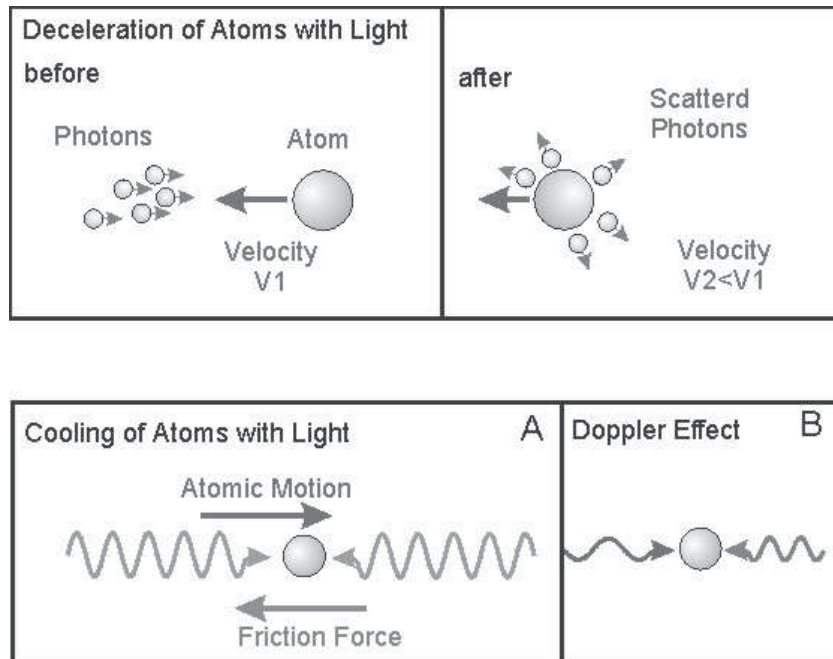


Figure 114: Schematics of laser cooling

Assume a moving atom is interacting with monochromatic laser which is red detuned from the resonance of an electronic transition of the atom. Then, the atom can only absorb photons from the laser light if it moves towards the laser and is thus tuned to resonance by the Doppler shift. The atom experiences a momentum change Δp which causes a deceleration. After absorption the atom spontaneously emits the photon again. Since spontaneous emission is isotropic there is no momentum change *on the average*. Two laser beams from opposite directions can thus decelerate or cool the atomic motion in one direction. Accordingly, three pairs of laser beams establish a cooling in all three directions. The minimum temperature achievable in this way by *Doppler cooling* is the *Doppler temperature*:

$$k_B T_D = \frac{\hbar \Gamma}{2}$$

where Γ is the natural linewidth of the transition.

The achievable deceleration is remarkable: An atom moving with a thermal velocity of 1000 m/sec can be stopped within a ms. This correspond roughly to 10^5 g!

13.2.2 Harmonic potential

As pointed out above the trap potential for ions in a Paul trap is usually harmonic close to the trap's center. The Hamiltonian of a particle in a one dimensional harmonic potential is:

$$H = \frac{p^2}{2m} + \frac{1}{2}m\omega^2x^2$$

with the definition of the creation and annihilation operator a^\dagger, a

$$a = \frac{1}{\sqrt{2m\hbar\omega}}(m\omega x + ip)$$

$$a^\dagger = \frac{1}{\sqrt{2m\hbar\omega}}(m\omega x - ip)$$

with the properties

$$a^\dagger |n\rangle = \sqrt{n+1} |n+1\rangle$$

$$a |n\rangle = \sqrt{n} |n-1\rangle$$

one derives the Hamiltonian of the harmonic oscillator:

$$H = \hbar\omega \left(a^\dagger a + \frac{1}{2} \right)$$

The motional eigenstates of a trapped particle are thus harmonic oscillator eigenstates with equally spaced eigenvalues and sometimes similar as quantized lattice vibrations called *phonons*. The typical length scale x_0 is:

$$x_0 = \sqrt{\hbar/2m\omega}$$

13.2.3 Sideband Cooling

In a trap potential ions can be cooled down even further than the Doppler limit by the so-called **sideband cooling**. Figure 115 illustrates how this works:

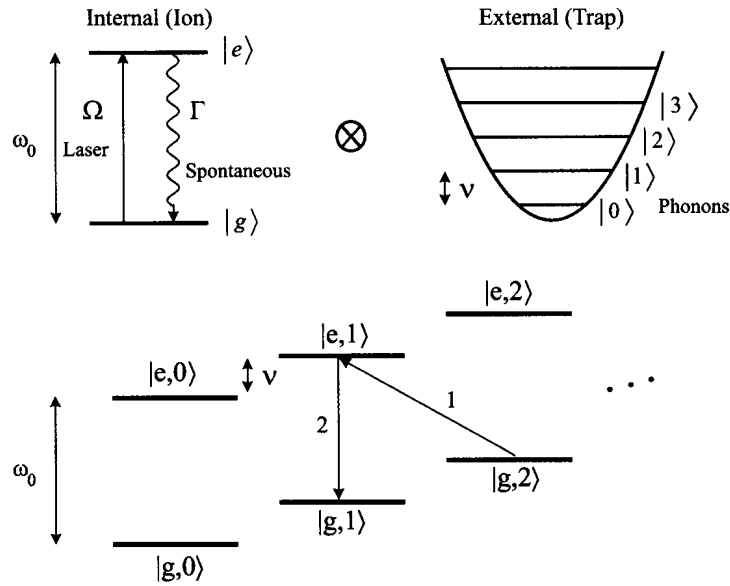


Figure 115: Schematics of sideband-cooling [from Bouwmeester et al.]

The lowest picture shows the typical energy structure of an ion in a trap. It is a combination of the ion's two internal states (e and g) and the motional states. A laser is tuned to a transition to an excited state with a lower motional excitation. Spontaneous emission now causes a transition without change of the motional state (on the average). Since the potential is harmonic this scheme applies to all pairs of neighboring motional states. Motional quanta are removed one-by-one in each optical cycle, and the ion ends up in the motional ground state which is then decoupled from the laser light.

In experimental realizations either a stabilized laser is used to resolve individual sidebands or a Raman transition where the energy difference between two incident lasers equals the energy of one phonon.

13.2.4 Choosing atoms

Although an ion trap is very deep (several eV potential well depth) and will hold almost every ion, only a few ions are suitable for quantum computation. The following

requirements should be met:

- The electronic level structure should be simple to allow the realization of a closed two level system without the need of too many lasers.
- The levels used for the qubit transition should have a negligible decoherence (e.g. by spontaneous decay).
- The levels should allow for efficient laser cooling and detection (some strong transitions).

Because of these requirements the ions of choice have typically only one electron in the outer shell (hydrogenic ions). The two level system can either be provided by *two hyperfine ground states* or by a *ground state and a long-lived metastable electronic state*.

Most of the experiments have been done with ${}^9\text{Be}^+$ and ${}^{40}\text{Ca}^+$, but other possible ions are ${}^{138}\text{Ba}^+$, ${}^{25}\text{Mg}^+$, ${}^{199}\text{Hg}^+$, and ${}^{171}\text{Yb}^+$.

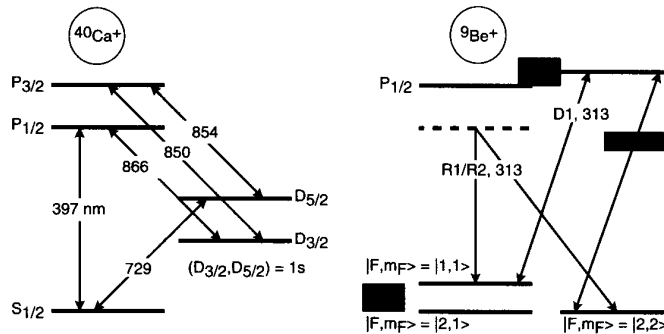


Figure 116: Energy levels of Ca and Be [from Bouwmeester et al.]

Cooling of the ions starts with Doppler cooling. In ${}^9\text{Be}^+$, the ultraviolet $S_{1/2} \rightarrow P_{3/2}$ transition at 313 nm is used, while for the ${}^{40}\text{Ca}^+$ the corresponding transition is 397 nm. Frequency doubled Ti:Sapphire or dye lasers are used to generate the UV light. (A major advantage of a specific ion could be whether it is possible to use cheap lasers, e.g. diode lasers for the optical excitations!)

The Doppler cooling leads to a thermal state of motion with a temperature of

about 1 mK . Then, it depends on the trap depth how many motional states n_{phonon} are occupied at this temperature. The number ranges between $\langle n_{phonon} \rangle = 1.3$ ($\omega_{trap}/2\pi = 11 MHz$) and $\langle n_{phonon} \rangle = 50$ ($\omega_{trap}/2\pi = 140 kHz$). Subsequent side-band cooling cools the ions to the motional ground state.

13.3 Quantum information gates with trapped ions

13.3.1 Hamiltonian of ions in a trap

The Hamiltonian of N ions in a 3-dimensional harmonic trap potential which interact via Coulomb interaction is:

$$H_{Nions} = \sum_{i=1}^N \frac{m}{2} \left(\omega_x x_i^2 + \omega_y y_i^2 + \omega_z z_i^2 + \frac{|p_i|^2}{2} \right) + \sum_{i=1}^N \sum_{i < j} \frac{e^2}{4\pi\epsilon_0 (\vec{r}_i - \vec{r}_j)}$$

Since a typical trap potential in a linear ion trap is shallowest in the z -direction (i.e. perpendicular to the end caps) it is sufficient here to consider only the z -coordinate. The ions remain in the ground state with respect to the oscillation in both x - and y -direction.

The ions are laser cooled to the so-called *Lamb-Dicke regime*. The Lamb-Dicke regime is defined as $\eta \ll 1$, where η is the Lamb-Dicke parameter. This parameter gives the ratio between the typical length scale z_0 of an ion's oscillation amplitude in a harmonic trap potential and the wavelength λ of the incident laser radiation:

$$\eta = 2\pi z_0 / \lambda = 2\pi \sqrt{\hbar / 2Nm\omega_{trap}} / \lambda$$

where N is the number of ions in the trap, m the ion's mass, and ω_{trap} is the trap frequency.

If the ions are laser cooled they only perform small oscillations around their equilibrium position. Then the Coulomb potential can be expanded as a Taylor series. Thus, the potential (trap and Coulomb potential) along the z -direction can be written as:

$$V(z) = \sum_{i=1}^N \sum_{j=1}^N U_{ij} z_i z_j$$

The diagonalization of this potential can be achieved by transforming to the normal variables. Finally, the Hamiltonian H_{Nions} is transformed into

$$H_{Nions} = \sum_{i=1}^N \hbar\omega_i a_i^\dagger a_i$$

which is an harmonic oscillator potential for N *normal modes*.

13.3.2 Interaction with a laser field

The interaction of the ions in the trap with a classical laser field at frequency ω is now:

$$H_I^i = \Omega_i \cos(kz_i + \phi_i + \omega t)(\sigma_i^+ + \sigma_i^-)$$

Note here that we considered one particular normal mode i and assumed a standing wave laser field. The Rabi-frequency Ω_i is proportional to the amplitude of the classical laser field. σ_i^+ and σ_i^- describe the raising and lowering operators of the atom's two internal states.

The coordinate z_i is now quantized due to the motion in the trap potential:

$$z_i = z_{i,equilibrium} + 1/\sqrt{\hbar/2Nm\omega_{CM}}(a + a^\dagger)$$

Note: We consider only an excitation of the lowest (center-of-mass) normal mode. This introduces the factor of $1/\sqrt{N}$ to the normal coordinates. With the equilibrium position absorbed in the phase ϕ_i the Hamiltonian reads:

$$H_I^i = \Omega_i \cos\left(\frac{\eta}{\sqrt{N}}(a + a^\dagger) + \phi_i + \omega t\right)(\sigma_i^+ + \sigma_i^-)$$

In the limit of small Lamb-Dicke parameter, $\eta \ll 1$, one finds after some algebra two cases:

1. Laser tuned to the internal atomic transition $\omega = \omega_0$:

$$H_I^i = \Omega_i/2 (\sigma_i^+ \exp(i\phi_i) + \sigma_i^- \exp(-i\phi_i))$$

The laser field introduces only transitions between internal states of the ions.

2. Laser tuned to one of the sideband transitions $\omega = \omega_0 \pm \omega_{CM}$:

$$H_I^i = \frac{\Omega_i}{2\sqrt{N}} (\sigma_i^+ a^\dagger \exp(i\phi_i) - \sigma_i^- a \exp(-i\phi_i)) \quad \text{if } \omega = \omega_0 + \omega_{CM}$$

$$H_I^i = \frac{\Omega_i}{2\sqrt{N}} (\sigma_i^+ a \exp(i\phi_i) - \sigma_i^- a^\dagger \exp(-i\phi_i)) \quad \text{if } \omega = \omega_0 - \omega_{CM}$$

In this case, in addition to an internal transition one phonon is created or annihilated.

The following figure shows a sketch of the different possibilities:

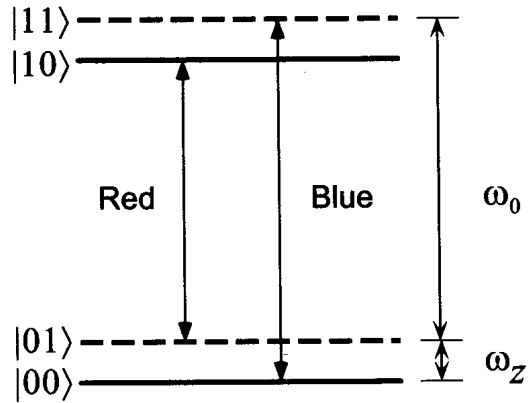


Figure 117: Schematics of possible transitions in a trapped ion [from Nielsen and Chuang]

13.3.3 Single qubit operation

A qubit is encoded in the internal states of the ions:

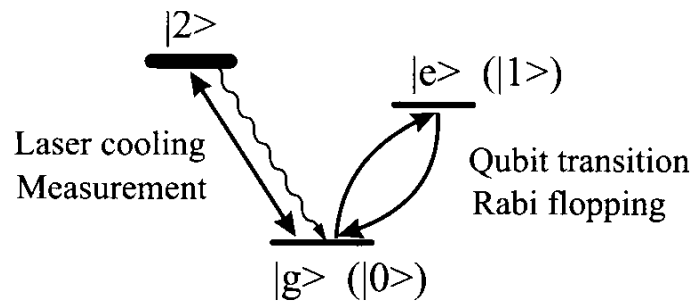


Figure 118: Encoding qubits in a trapped ion [from Bouwmeester et al.]

Single qubit gates are established by tuning the laser to the frequency $\omega = \omega_0$. By choosing the phase shift ϕ and the duration of the interaction appropriately, arbitrary rotations can be performed. Thus, any single qubit-gate can be realized this way.

13.3.4 Two qubit operation

A controlled phase-flip gate can be constructed with the help of an auxiliary atomic level in the following way [J. I. Cirac, P. Zoller, Phys. Rev. Lett. 74, 4091 (1995)]:

ie.

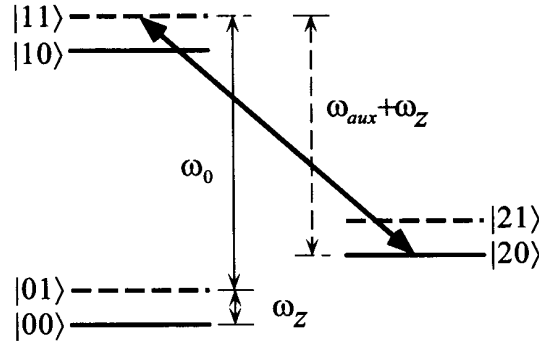


Figure 119: Schematics of a two qubit gate [from Nielsen and Chuang]

1. We first assume that initially one qubit is stored in an ions internal state ($|0\rangle$, or $|1\rangle$), another qubit is stored in the phonon state ($|0\rangle$, or $|1\rangle$). Both qubits can be in any arbitrary superposition.
2. A laser is tuned to the frequency $\omega_{aux} + \omega_z$, to cause the transition between the auxiliary state $|20\rangle$ and only the state $|11\rangle$. Because of the uniqueness of this frequency, no other transitions are excited. The phase and duration of the laser pulse is chosen properly to make a 2π -pulse. This results in

$$|11\rangle \longrightarrow -|11\rangle$$

All other states remain unchanged. Thus the effect on the initial state is:

$$\begin{aligned} (|0\rangle + |1\rangle)_{ion}(|0\rangle + |1\rangle)_{phonon} &= |00\rangle + |10\rangle + |01\rangle + |11\rangle \\ &\longrightarrow |00\rangle + |10\rangle + |01\rangle - |11\rangle \end{aligned}$$

which is the desired controlled phase gate.

3. In order to decode both qubits in ions a SWAP-gate is required which maps an ions qubit state on a phonon qubit state. This can be done by tuning the laser to the frequency $\omega_0 - \omega_z$, and arranging the phase and pulse duration such that a π -pulse is established:

$$(\alpha|0\rangle + \beta|1\rangle)_{ion} \longrightarrow (\alpha|0\rangle + \beta|1\rangle)_{phonon}$$

The interaction between arbitrary qubits is achieved since the phonons are quantized modes of the *center-of-mass* (COM) oscillation shared by all ions in the trap! The COM-mode acts as a *quantum bus* as sketched in the following cartoon:

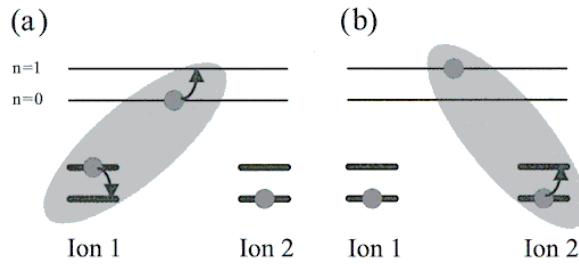


Figure 120: Quantum computation with trapped ions [from Bouwmeester et al.]

A CNOT gate between ion k and ion j can thus be constructed using the following sequence of operations:

$$CNOT_{jk} = H_k \overline{SWAP}_k C_j SWAP_k H_k$$

where C_j is the controlled phase gate on the ion j and H_k are Hadamard gates on ion k .

Any quantum computation can thus be performed with a string of trapped ions!

More recent proposals [J. F. Poyatos, J. I. Cirac, P. Zoller, Phys. Rev. Lett. 81, 1322 (1998)] show that clever techniques exist to perform a quantum computation with somewhat hotter ions, which don't have to be cooled to the Lamb-Dicke regime by Doppler and sideband cooling. For these techniques Doppler cooling alone may be sufficient.

13.4 Experimental Realization of a CNOT Gate

A first demonstration of a CNOT gate was demonstrated in the group of D. Wineland at NIST, Boulder, USA [C. Monroe et al., Phys. Rev. Lett. 75, 4715 (1995)].

(See also <http://www.bldrdoc.gov/timefreq/ion/index.htm>) A single ${}^9\text{Be}^+$ ion was trapped and laser cooled into the motional ground state. The computational basis was:

$$|0\rangle|\uparrow\rangle, |0\rangle|\downarrow\rangle, |1\rangle|\uparrow\rangle, \text{ and } |1\rangle|\downarrow\rangle$$

where $|0\rangle$ and $|1\rangle$ denote the motional states and $|\uparrow\rangle$ and $|\downarrow\rangle$ the internal (hyperfine states). More precisely:

$$\begin{aligned} |\uparrow\rangle &= {}^2S_{1/2} |F=2, m_F=2\rangle \\ |\downarrow\rangle &= {}^2S_{1/2} |F=1, m_F=1\rangle \end{aligned}$$

An additional state was used as auxiliary state,

$$|aux\rangle = {}^2S_{1/2} |F=2, m_F=0\rangle$$

another state was used for detection:

$${}^2P_{3/2} |F=3, m_F=3\rangle$$

The following shows the level scheme and a miniaturized Be-ion trap:

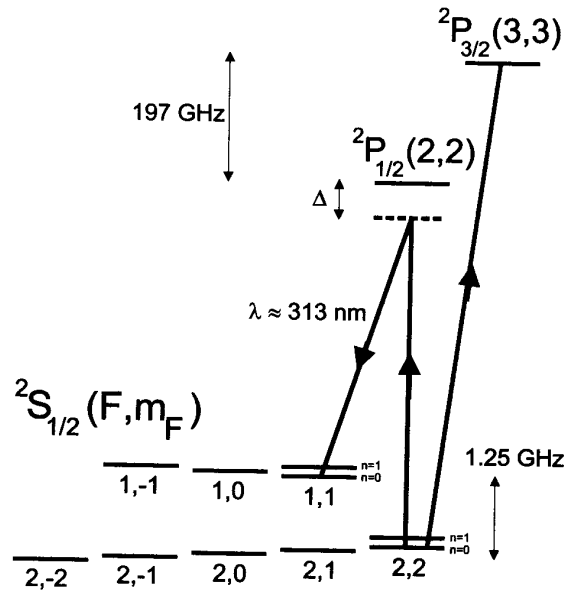


Figure 121: Energy levels of a Be-ion used for experimental demonstration of a CNOT gate [from Bouwmeester et al.]

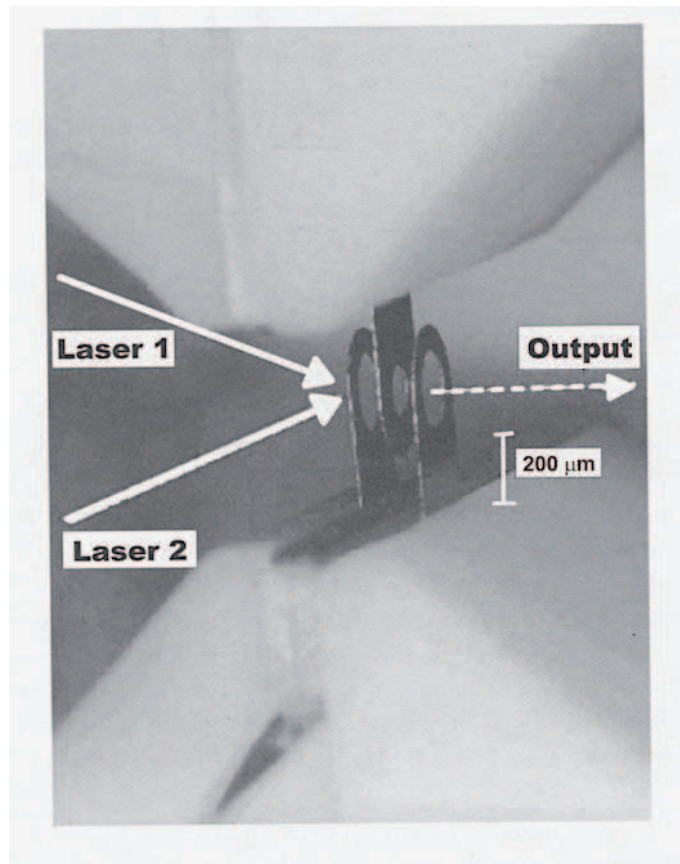


Figure 122: Picture of a miniaturized ion trap [from Nielsen and Chuang]

In order to demonstrate a CNOT gate the following procedure was used:

1. Doppler and sideband cooling of the ion in the $|0\rangle|\downarrow\rangle$ state (95% probability).
2. Initialization in one of the four basis states $|0\rangle|\downarrow\rangle$, $|0\rangle|\uparrow\rangle$, $|1\rangle|\uparrow\rangle$, or $|1\rangle|\downarrow\rangle$ using single qubit rotations.
3. $\pi/2$ -pulse on the internal state. This leaves the motional state unchanged.
4. π -pulse on the $|1\rangle|\uparrow\rangle \rightarrow |aux\rangle$ transition. All other states remain unchanged.
5. $-\pi/2$ -pulse on the internal state. This leaves the motional state unchanged.
6. Detection of the population in the $|0\rangle|\downarrow\rangle$ and $|1\rangle|\downarrow\rangle$ states by shining σ^+ -polarized light resonant to the ${}^2P_{3/2}$ transition. This measures the internal qubit.

7. Swapping the motional and internal qubit. Then repeat step 6. This measures the motional qubit.

It is easy to verify that the steps 3 to 5 implement a CNOT gate. The following shows the measured CNOT true table:

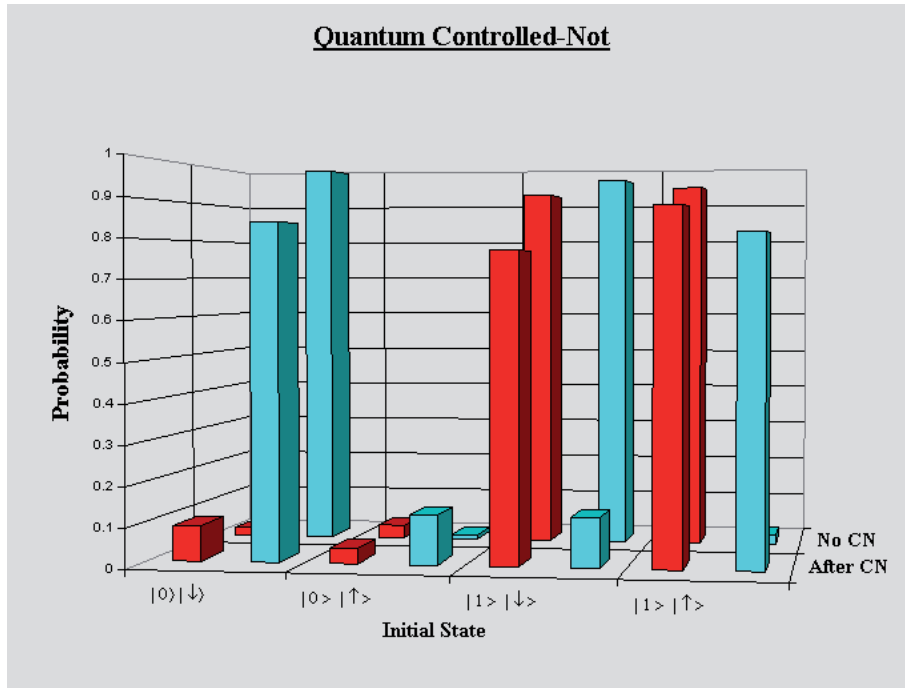


Figure 123: Experimental data of true table for a CNOT gate. [from <http://www.bldrdoc.gov/timefreq/ion/index.htm>]

In order to show that a CNOT gate could be performed on a coherent superposition of qubits with the coherence maintained, the detuning of the $\pi/2$ -pulses was changed. The following shows the resulting so-called Ramsey-fringes for the $|0\rangle|\downarrow\rangle$ and $|1\rangle|\downarrow\rangle$ states.

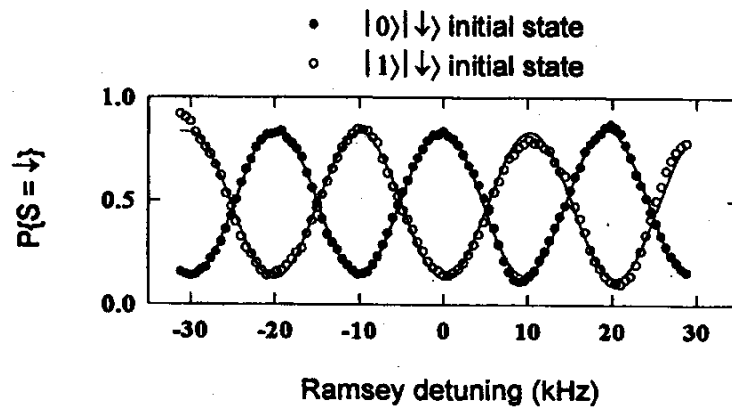


Figure 124: Ramsey spectra of the CNOT gate [from Monroe et al., Phys. Rev. Lett. 75, 4714 (1995)]

The time for the CNOT operations was about 50 microseconds with a measured decoherence time of milliseconds. the main source of decoherence was due to instabilities in the laser intensity, the RF fields and magnetic fields.

13.5 Gates and Tricks with Single Ions

First quantum computing algorithms have been realized, such as the Deutsch-Jozsa algorithm in the Innsbruck group [S. Gulde et al., Nature 421,48 (2003)]. Presently, it is possible to manipulate and individually control up to 10 ions in an ion trap. Quantum teleportation of an unknown quantum state to another was demonstrated by the Innsbruck group [M. Riebe et al., Nature 429, 734 (2004)] and Boulder group [M. D. Barret et al., Nature 429, 737 (2004)]. Also a quantum byte [Häffner et al., Nature 438, 643 (2005)] and a 6-ions GHZ entangled state [D. Leibfried et al., Nature 438, (2005)] were created. In order to obtain even more complex elements novel miniturized ion traps are being developed.

13.5.1 Demonstration of Deutsch-Jozsa

This algorithm was demonstrated by using two qubits. One qubit was implemented in the ground and a metastable state of Ca ions, the $S_{1/2}$ - and $D_{5/2}$ -state respectively. The following picture shows the energy diagramme.

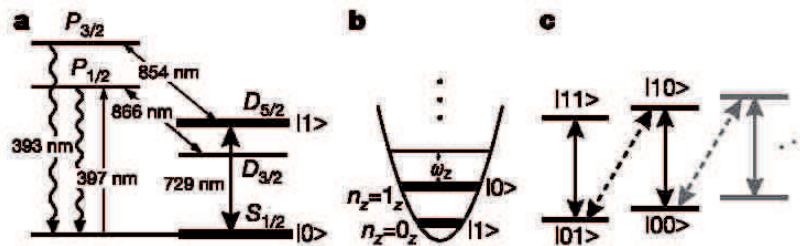


Figure 125: Qubits in the experimental demonstration of the two-qubit Deutsch-Jozsa algorithm [from S. Gulde et al., Nature 421,48 (2003)].

The algorithm (including the function U_f) was encoded by using different laser pulses. Laser frequencies could be tuned with the help of acousto-optic modulators. The following figure shows the probability to find the ion in the upper atomic qubit state. In order to derive this probability the procedure was repeated many times and interrupted after a certain time had elapsed. The experiment shows that it is indeed possible to control a single ion in an ion trap with very high precision. For more complex algorithms the application of the laser pulses will be controlled by a computer. This somewhat approaches techniques which already exist in nuclear magnetic resonance experiments for microwave pulses.

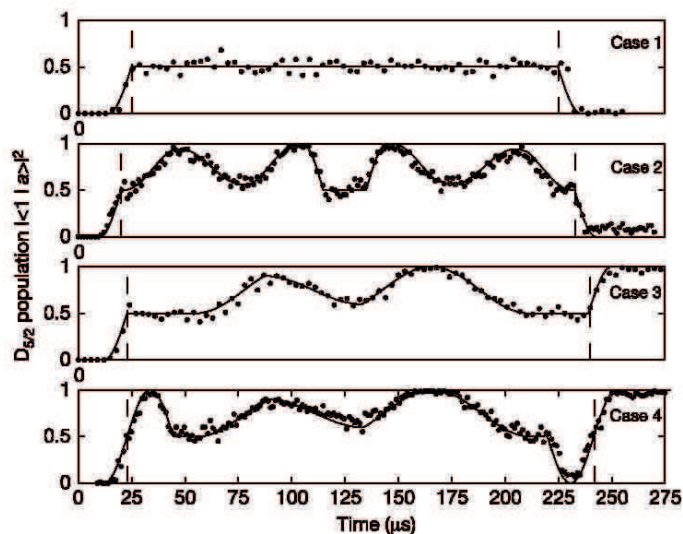


Figure 126: Time evolution of the population of the upper atomic qubit for four different encoded functions [from S. Gulde et al., Nature 421,48 (2003)].

13.5.2 Teleportation of atomic qubits

A recent progress was the demonstration of teleportation of an atomic state from one trapped ion to another. In the Innsbruck group led by Rainer Blatt [M. Riebe et al., Nature 429, 734 (2004)] three ions were manipulated with carefully designed laser pulses. Individual ions could be prevented from disturbance due to detection light by applying so-called "hide"-pulses, which transferred the state to another Zeeman level. The following picture shows the diagram of the algorithm.

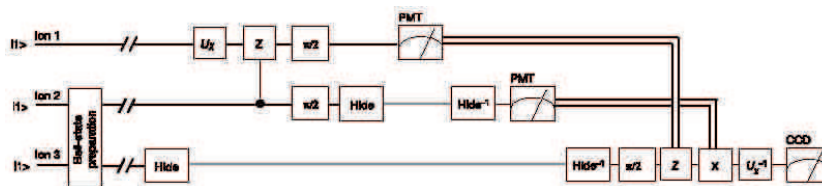


Figure 127: Diagram of the teleportation scheme implemented with three ions [from M. Riebe et al., Nature 429, 734 (2004)].

The implementation of the algorithm consisted of 35 laser pulses including spin echo pulses to revert dephasing. This clearly demonstrates that computer control is essential for an upscaling to more qubits. The following pictures shows the fidelities

for teleportation of different quantum states.

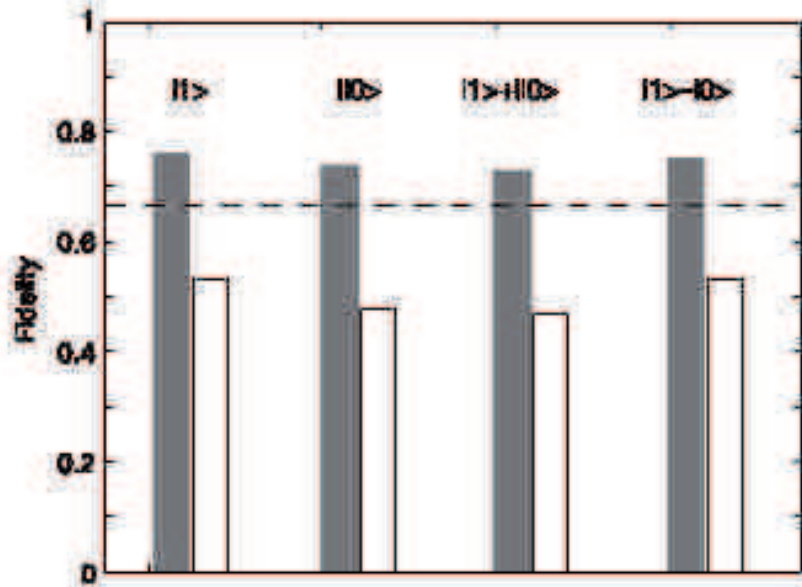


Figure 128: Experimental results for the teleportation of different quantum states [from M. Riebe et al., Nature 429, 734 (2004)].

The group in Boulder led by Dave Wineland followed a slightly different approach. They used a miniaturized ion trap which allowed to move ions from one segment to another. In this way it was also possible to address individual ions with laser pulses. Qubits were encoded in two hyperfine levels of Be ions.

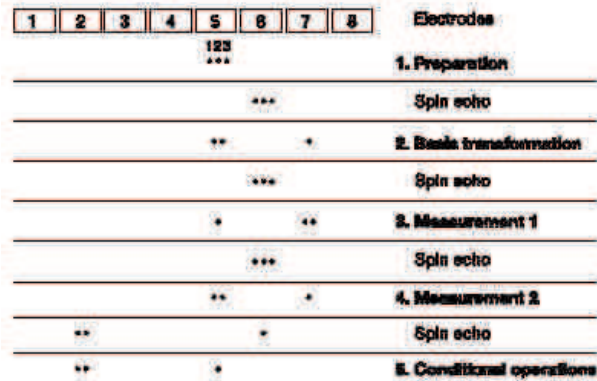


Figure 129: Schematics of the minitimized ion trap and the position of the different ions during the teleportation sequence [from M. D. Barret et al., Nature 429, 737 (2004)].

In order to demonstrate successful teleportation of arbitrary states a Ramsey interference was measured by applying pulses to ion 1 before and to ion 3 after teleportation.

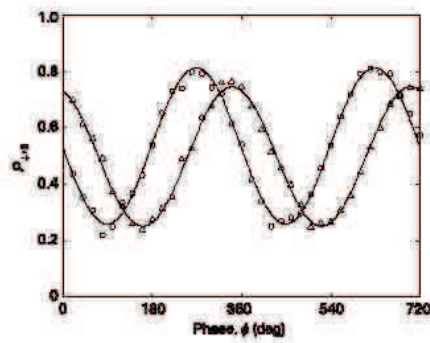


Figure 130: Measured Ramsey interference by applying pulses to ion 1 before and to ion 3 after teleportation for two different phases of the second Ramsey pulse. [from M. D. Barret et al., Nature 429, 737 (2004)]

13.5.3 A Quantum Byte

Linear ion straps allow to trap and cool a large number of atoms. An experimental challenge is to manipulate all trapped ions precisely with tailored laser pulses. Recently, the Innsbruck groups realized a *quantum byte*, i.e., an arbitrary quantum state consisting of 8 quantum bits [Häffner et al., Nature 438, 643 (2005)].

As an example for a complex multi-particle qubit state a *W-state* or *Werner-state* was created. Such a state has a single excitation (one ion in an excited state), but there is no information in which ion.

$$|W_N\rangle = |10000000\rangle + |01000000\rangle + \dots |00000001\rangle$$

In the experiment the 0- and 1-state were realized as the $S_{1/2}$ ground state and the $D_{5/2}$ metastable state in ^{40}Ca -ions. First, all ions were prepared in the state:

$$|W_N\rangle = |0, DDDDDDDD\rangle$$

where the first 0 denotes the motional ground state of center of mass oscillation. Then, ion 1 is flipped by a π -pulse on the carrier transition to

$$|W_N\rangle = |0, SDDDDDDD\rangle$$

Then, most of the population is moved to the $|W_N\rangle = |1, DDDDDDDD\rangle$ state by applying a blue sideband pulse of length $\theta_n = \arccos(1/\sqrt{n})$:

$$\frac{1}{\sqrt{N}}|0, SDDDDDDD\rangle + \frac{\sqrt{N-1}}{\sqrt{N}}|1, DDDDDDDD\rangle$$

This procedure is continued until the final state is reached:

$$|W_N\rangle = \frac{1}{\sqrt{N}}|0, SDDDDDDD\rangle + \frac{1}{\sqrt{N}}|0, DSDDDDDD\rangle + \dots \\ + \frac{1}{\sqrt{N}}|0, DDDDDDDS\rangle$$

The entangled procedure took about 1 *ms*. A major problem is to gain full information of the N-ion complex quantum state. This was obtained via *quantum state reconstruction* by expanding the density matrix in a basis of observables and measuring the corresponding expectation values. In order to do this, a large number (about 650000) additional laser pulses were employed. A full characterization of the state required 10 hours measurement time. A fidelity exceeding 70% were obtained (see reconstructed density matrix in Fig. 131).

The experiment demonstrates that presently there is not only a limit with respect to constructing a complex quantum state, but also to characterize is to full extend, not to mention to perform a tomography of a whole complex quantum gate.

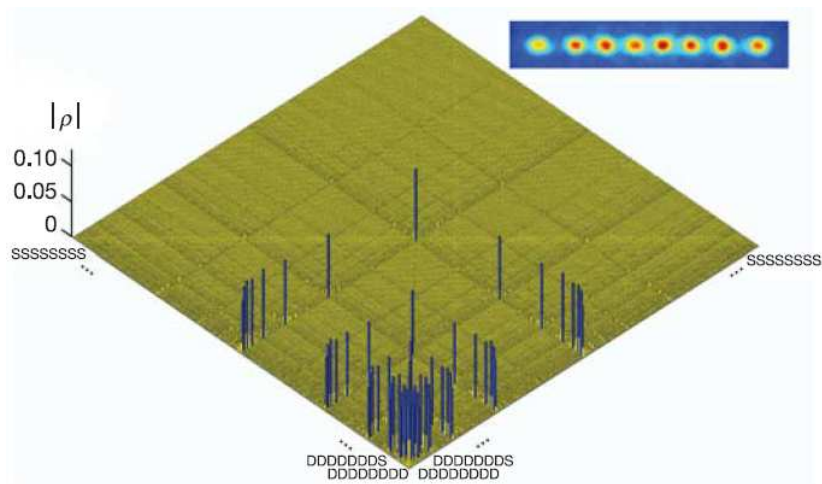


Figure 131: Absolute values, $|\rho|$, of the reconstructed density matrix of a W-state as obtained from quantum state tomography. DDDDDDD...SSSSSSSS label the entries of the density matrix ρ . Ideally, the blue coloured entries all have the same height of 0.125; the yellow colored bars indicate noise. In the upper right corner a string of eight trapped ions is shown. [Häffner et al., Nature 438, 643 (2005)]

13.5.4 Novel Trap Designs

The problem of ion traps as quantum computing devices is their complexity. Ion traps have to be implemented in rather large ultra-high vacuum chambers. The required equipment for lasers and laser control is demanding as well. Figure 132 shows part of the experimental setup (mainly the vacuum chamber), and Fig. 133 a close-up of a linear ion trap.

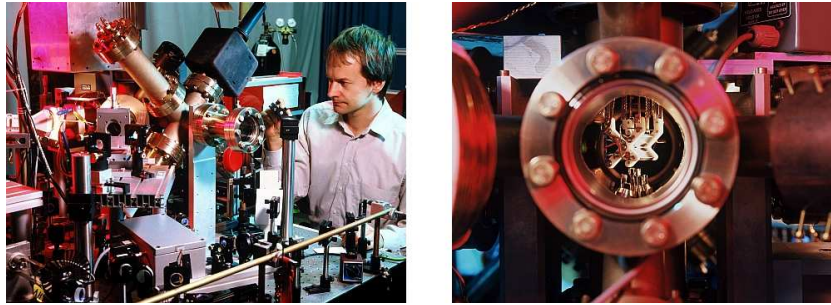


Figure 132: Left: Part of the setup of the ion trap experiment in Innsbruck. Right: Look inside the ultra-high vacuum chamber [from <http://heart-c704.uibk.ac.at/>].



Figure 133: Close-up of a linear ion trap [from <http://heart-c704.uibk.ac.at/>].

A solution to reduce the complexity of ion-trap experiment is to develop miniaturized ion-traps, or *micro-traps* (similar approaches are pursued with traps for neutral atoms as well). Figure 134 shows a standard linear ion trap with four rods together with a layered design suitable for miniaturization. An even simpler design is displayed in Fig. 135.

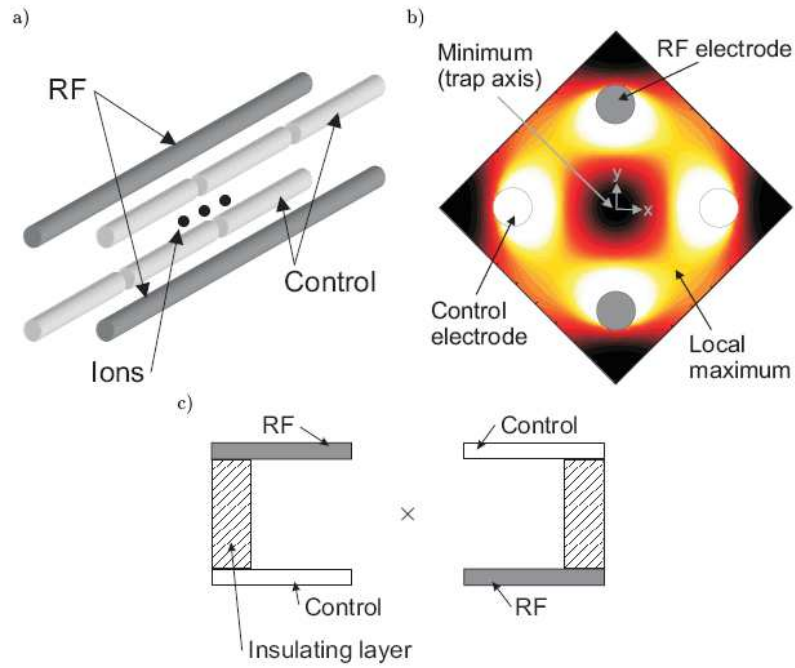


Figure 134: a: Standard four-rod ion trap; b: radial pseudopotential contours; c: Implementation of four-rod design using a layered structure [Chiaverini et al., *Quant. Inf. and Comp.* 5, 419 (2005)].

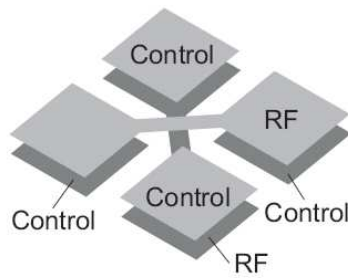


Figure 135: Schematic diagram of a modified two-layer cross to maintain a trapping potential at the center of the cross [Chiaverini et al., Quant. Inf. and Comp. 5, 419 (2005)].

Minaturized surface traps are combined with miniaturized waveguides/antenna for RF radiation required for Paul traps and integrated on chips using standard procedures. Figure 136 shows such a *atom chip*.

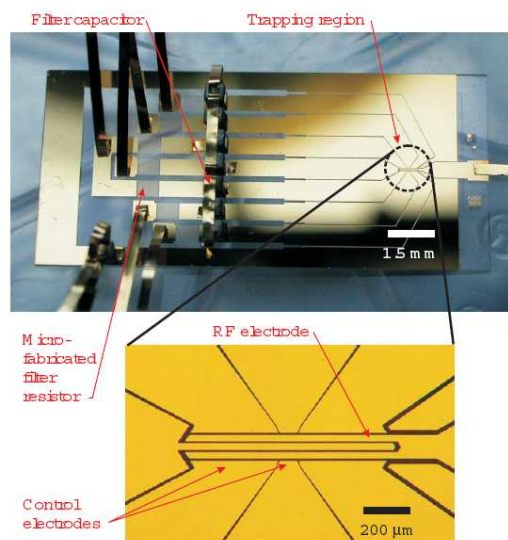


Figure 136: Micrograph of a five wire, one-zone linear trap fabricated of gold on fused silica. The top figure is an overview of the trap chip showing contact pads, onboard passive filter elements, leads, and trapping region. The lower image shows a detail of the trapping region [Chiaverini et al., Quant. Inf. and Comp. 5, 419 (2005)].

It is indeed possible to trap ions on atom chips and to manipulate them in a controlled way (see Fig. 137). A problem is that ions couple strongly to charges and charge fluctuations. Thus, close to surfaces there is an increased heating and decoherence rate which makes it more difficult to maintain coherent operations.

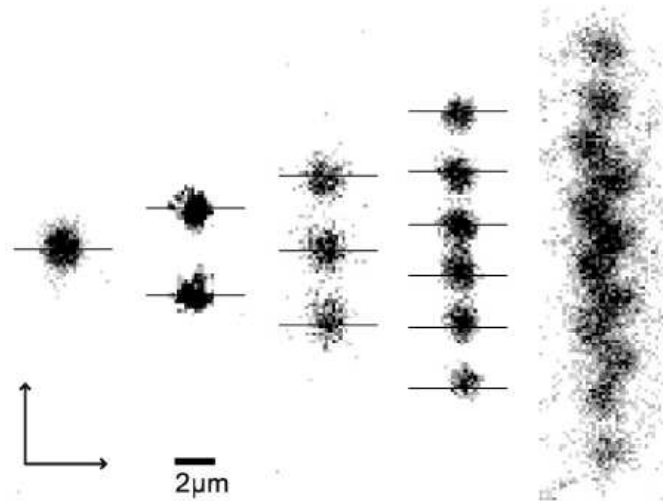


Figure 137: Images of 1, 2, 3, 6, and 12 ions confined in a surface-electrode trap. The length scale is determined from a separate image of the electrodes whose dimensions are known. The horizontal bars indicate the separation distance between the ions as predicted from the measured axial oscillation frequency. The ratio between transverse and axial oscillation frequencies makes it energetically favorable for the 12 ion string to break into a zigzag shape [S. Seidlin et al., PRL 253003 (2006)]

Figure 138 displays another design for a minaturized ion trap. It can be implemented in a standard chip holder to connect all required electrodes (see Fig. 139).

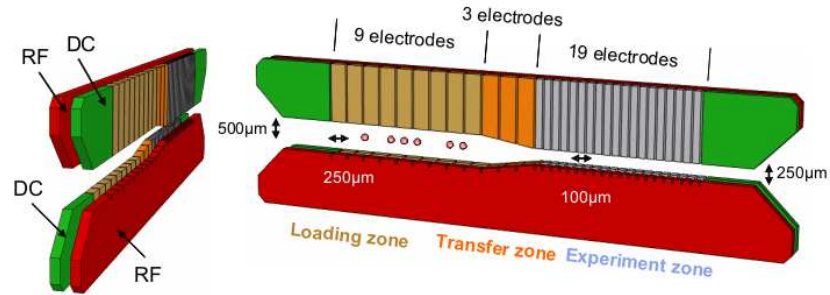


Figure 138: Trap geometry of a minaturized linear ion trap [courtesy F. Schmidt-Kaler].

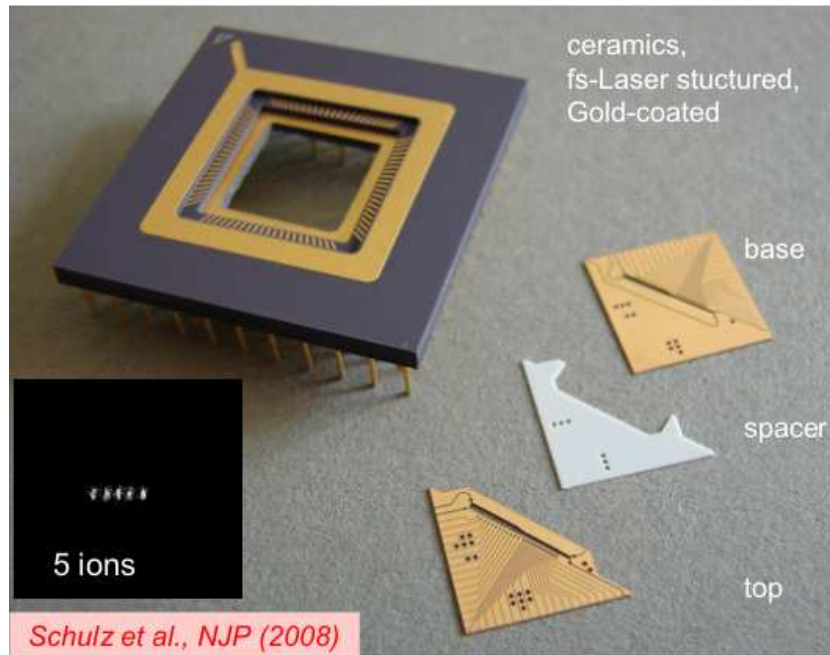


Figure 139: Components for assembling a minaturized ion trap in a chip holder. The inset shows a photo of five trapped ions [courtesy F. Schmidt-Kaler].

There are theoretical proposals how efficient quantum computing can be performed with a large number of ions in minaturized ion traps using only a few ions at a time [Kielpinsky et al., Nature 417, 709 (2002)]. This requires transferring ions to specific locations on an atom chip.

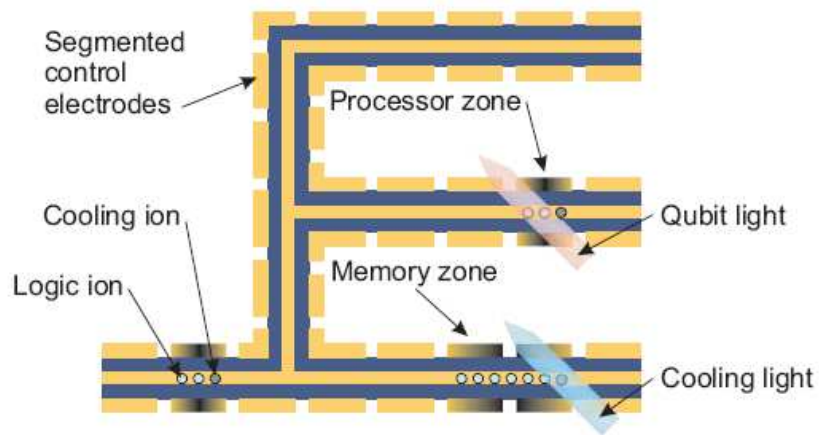


Figure 140: Schematic diagram of a proposed large-scale ion trap array for quantum information processing. Segmented control electrodes allow logic ions (lighter-colored circles) to be transferred to memory and processor regions. After transport ions are recooled by sympathetic cooling (darker-colored circles). [Chiaverini et al., Quant. Inf. and Comp. 5, 419 (2005)]

13.6 Ion trap Cavity QED Systems

One of the problems in the cavity QED-systems introduced in the previous chapters was that the qubits were *flying* qubits (atomic beams were used!). In order to solve this problem there are now attempts to use stored ions in combination with optical cavities.

Two groups in Munich and Innsbruck have successfully stored ions in an ion trap inside high-Q optical cavities.

The Innsbruck group experimentally examines the interaction of a single trapped Calcium ion with a single mode of radiation in a high finesse cavity resonant with the $S_{1/2} - D_{5/2}$ quadrupole transition of the ion. The following pictures show the experimental setup.



Figure 141: Experimental setup of the ion trap cavity-QED experiment in Innsbruck [from <http://heart-c704.uibk.ac.at/>]

The Munich group have successfully demonstrated that they can place a single trapped Calcium ion at will inside an optical resonators [G. Guthohrlein et al., *Nature*, 414, 49 (2001)]. The following pictures show a sketch of the experimental setup and a measurement of fluorescence from the ion. Depending on the position of the ion inside the cavity, the ion is in interaction with a node or an antinode of the standing wave cavity field. Thus, the amount of detected fluorescence light reflects the mode structure of the cavity.

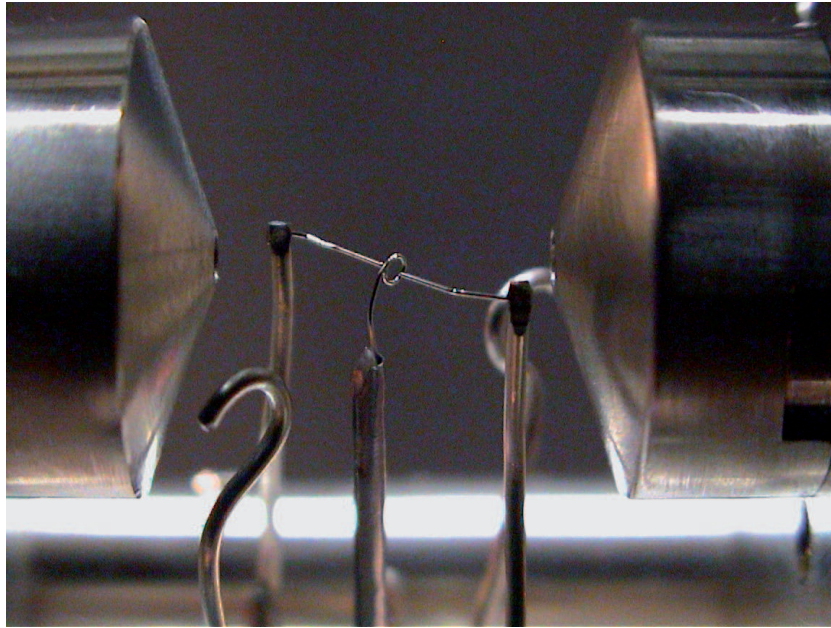


Figure 142: Photo of a Paul trap inside an optical resonator [from <http://heart-c704.uibk.ac.at/>]

It may be very difficult to achieve interaction of many ions with a single or a few modes in such setups. However, these systems may be promising candidates for smaller scale quantum interfaces, where quantum information is stored or manipulated in ions, then transferred to photons, and transmitted to other interfaces. The following shows a sketch of one building block of such a quantum network:

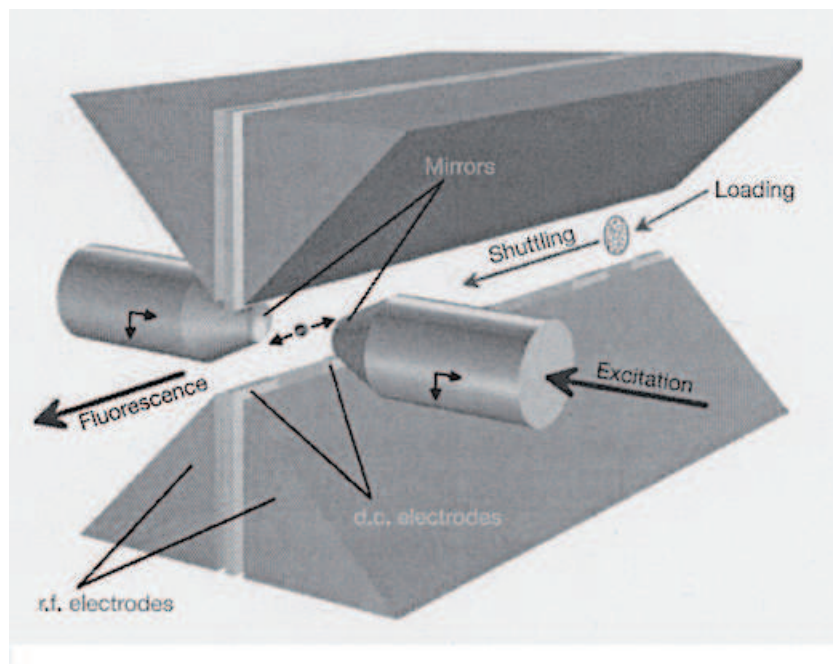


Figure 143: Sketch of the experimental setup in the Munich experiment [from Guthörlein et al., Nature 414, 49 (2001)]

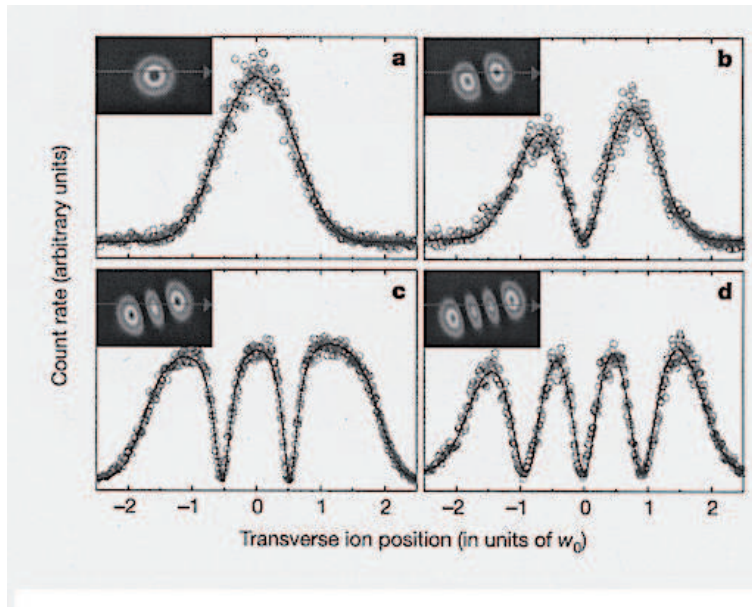


Figure 144: Scattered light from a single trapped Ca-ion in an optical cavity [from Guthörlein et al., Nature 414, 49 (2001)]

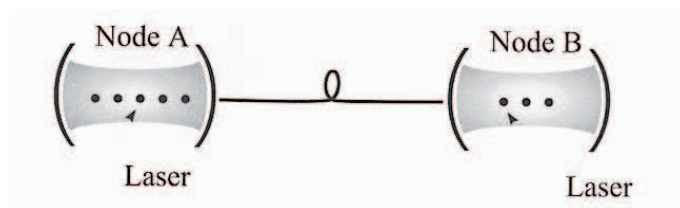


Figure 145: Sketch of a possible quantum network using cavity-QED systems with trapped ions [from Bouwmeester et al.]